



GEOLOGICAL SURVEY OF CANADA

OPEN FILE 4660

A Summary of the 2002 Sable Island Bank Hydrodynamic and Bedform Data

C. Smyth, M.Z. Li and D.E. Heffler

2004

This document was produced
by scanning the original publication.

Ce document est le produit d'une
numérisation par balayage
de la publication originale.

GEOLOGICAL SURVEY OF CANADA

OPEN FILE 4660

**A Summary of the 2002
Sable Island Bank Hydrodynamic and Bedform Data**

Carolyn Smyth, Michael Z. Li,
and Dave E. Heffler

2004

©Her Majesty the Queen in Right of Canada 2004
Available from
Geological Survey of Canada (Atlantic)
1 Challenger Drive
Dartmouth, Nova Scotia B2Y 4A2
Price subject to change without notice

Carolyn Smyth, Michael Z. Li and Dave E. Heffler, 2004:
A Summary of the 2002 Sable Island Bank Hydrodynamic and Bedform Data,
Geological Survey of Canada, Open File 4660, 18 p.

Open files are products that have not gone through the GSC formal publication process.

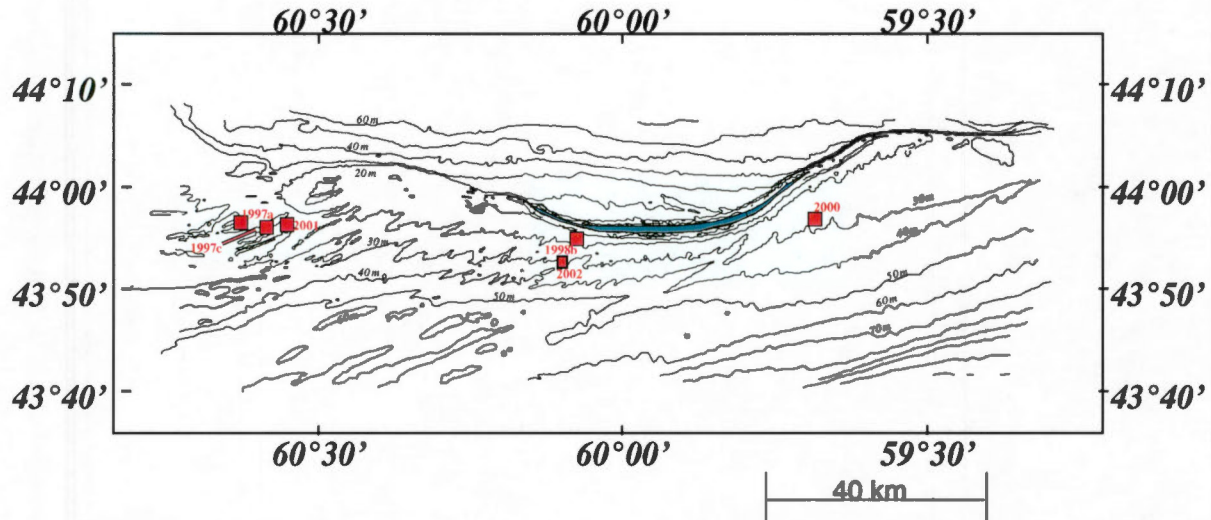


Figure 1: Bathymetry around Sable Island and the location of recent deployments. The 2002 site is just south of Sable Island on the western side.

1 Introduction

A joint project between the Geological Survey of Canada and Exxon-Mobil Canada (formerly Sable Offshore Energy Project) was initiated in 1999 to study sand ridge morphodynamics on Sable Island Bank. One of the goals of this project is to investigate the interaction between bottom boundary layer dynamics and sediment transport. In order to reach this goal, detailed measurements of flow dynamics and sediment transport modes have been collected.

This report summarizes the 2002 experiment which deployed instrumented frames approximately 10 km south of Sable Island about 5 km east of the Thebaud hydrocarbon production platform. Measurements include wave and current velocities, seafloor videos, and suspended sediment profiles. These measurements are analyzed to determine the magnitude and direction of sediment transport during storm conditions. Detailed scientific interpretations of these data will be presented in subsequent scientific publications.

2 Experiment Summary

2.1 Instrument Location

Three frames were deployed along a sand-ridge transect on February 24, 2002, including two S4 current meter frames, and an autonomous quad frame called Ralph. Ralph was positioned on the slope of a 0(10 m) high sand ridge in 31 m water depth (Figure 1). Two S4 frames were placed to the east of Ralph along a transect of the sand ridge with Ralph in the western trough, an S4 on the crest (S4C) and a second S4 in the eastern trough (S4T). Frame locations are given in Table 1. Surficial sediment samples from a van Veen grab sample at the Ralph location had a median grain diameter of 440 μm .

2.2 Instrumentation

Instruments on Ralph estimate water depth, wave velocity, current velocity, suspended sediment levels, and bedform dimensions. Table 2 briefly summarizes the instrumentation on Ralph, but a more thorough

Table 1: Instrument frame locations for the 2002 deployment. The instruments are abbreviated as follows: EMCM, Electro-magnetic Current Meter; OBS, Optical Backscatter Sensor; ABS, Acoustic Backscatter Sensor; and DV Camera, Digital Video Camera. The Imagenex are rotary sonars.

Frame Instruments		Latitude	Longitude
S4T	S4 (S/N 1590)	43° 52.839' N	60° 5.606' W
S4C	S4, OBS (S/N 2195)	43° 52.880' N	60° 5.737' W
Ralph	6 OBS, Pressure, Tilt, Temperature, 4 EMCM, 2 ABS, 2 ADV, Compass	43° 52.881' N	60° 6.122' W
	DV Camera, 2 Imagenex		

Table 2: Instrument descriptions and positions on the Ralph frame

Sensor	Resolution	Brand	Serial Number (X,Y,Z) [cm]	Position	Computer and Drive
Pressure Sensor	500 psi, 8.2 cm/bit	Data Inst. Model AB	0,0,162		TT7 120 Mb
Compass/Tilt	0.3 deg	Precision Nav. TCM2			
4 EMCM's	10 ft/s	Marsh McBirney	33 66 S758 T54	75,-53,26 7,-49,49 95,-52,66 111,-53,97	TT5F
6 OBS	20X gain	SeaPoint Inst.	brown red orange yellow green blue	6,-130,10 6,-130,30 6,-130,49 6,-130,66 6,-130,96 6,-130,119	
2 ABS	1 cm bins, 1 MHz	Mesotech	B2184 B2180	-31,64,133 -132,32,128	TT7 540 Mb
2 ADV	5 cm/s, 25 MHz	Sontek	B214 B216	-28,3,71 -133,-24,58	CF1, 1Gb
Pencil beam	1 cm bin, 0.675 MHz	Imagenex 881P	0609	-32,89,131	TT7 840 Mb
Fan beam	4 cm bin, 0.675 MHz	Imagenex 881I	0608	-158,88,158	
DV Camera	680 000 pixels, 5 lux	Sony TRV 15		-35,42,133	pic chip 60 min

description is given by *Heffler* [1996]. Six computers were used to control instruments, including a Tattletale 5F, 3 Tattletale 7's and 1 Compact Flash 1. Data were stored on 3 hard drives (a total of 2.6 Gb), and an additional 22 Gb camera tape. Instrument positions on the frame in Table 2 are given with respect to a reference origin, Figure 2, which indicates *x* and *y* directions for the current meters. The compass is aligned with the +*y* axis.

Two InterOcean S4 current meters were deployed to measure pressure, wave and current velocity, compass direction and optical backscatter amplitude. Each S4 sensor was mounted on an aluminum tubular frame 50 cm above the bed with an additional OBS sensor adjacent to the S4 at a height of 70 cm. S4C failed to record any data. The attempt to recover S4T was unsuccessful.

On the Ralph frame, the Imagenex pencil-beam had mechanical problems and did not rotate properly. Measured data has not yet been corrected for this problem. The Imagenex fan beam did not record any data.

Figure 2: Plan view of the Ralph frame showing instrument locations. Origin at pressure sensor location.

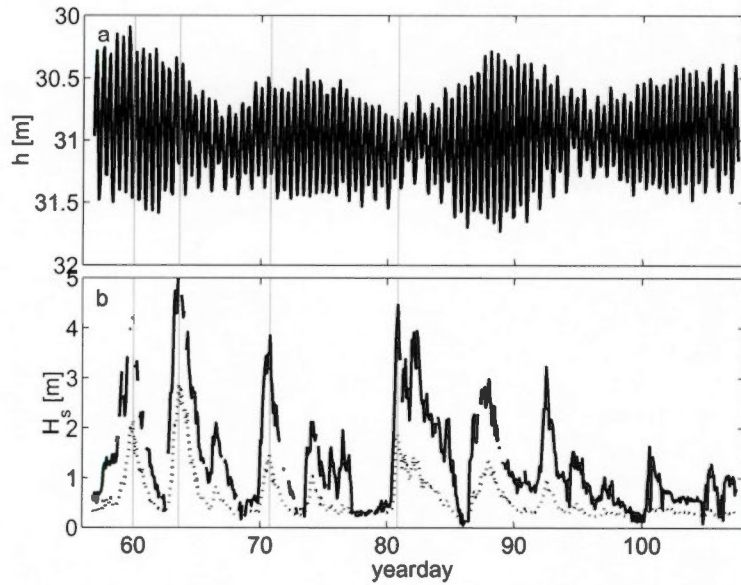
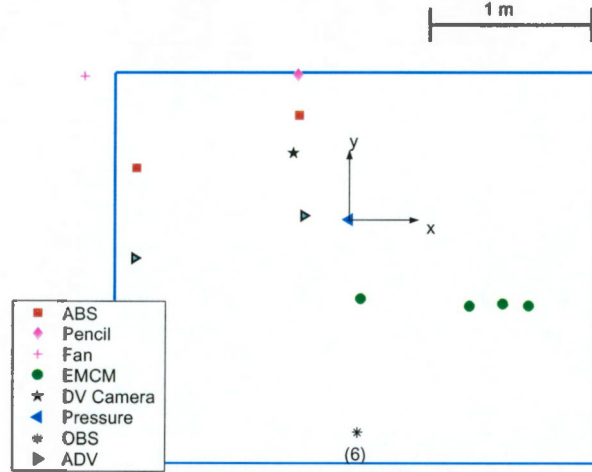


Figure 3: Time series of: (a) average water depth h , measured by the pressure sensor on Ralph and (b) the significant wave height, H_s , measured at depth (dashed) and corrected for attenuation.

2.3 Hydrodynamic Observations

Ralph was deployed on the slope of a sand ridge at the South Sable site. Burst-averaged water depth time series and significant wave height time series recorded by Ralph are shown in Figure 3. Four spring tides occurred during the deployment with a tidal range of approximately 1.3 m. Three neap tides had a tidal range of approximately 0.8 m.

Seven storm events were recorded during the deployment, with four storms having corrected significant wave heights greater than 3m, Figure 3b. Significant wave heights were corrected for depth attenuation of higher frequency wave energy. An energy threshold was applied at high frequencies to prevent noise

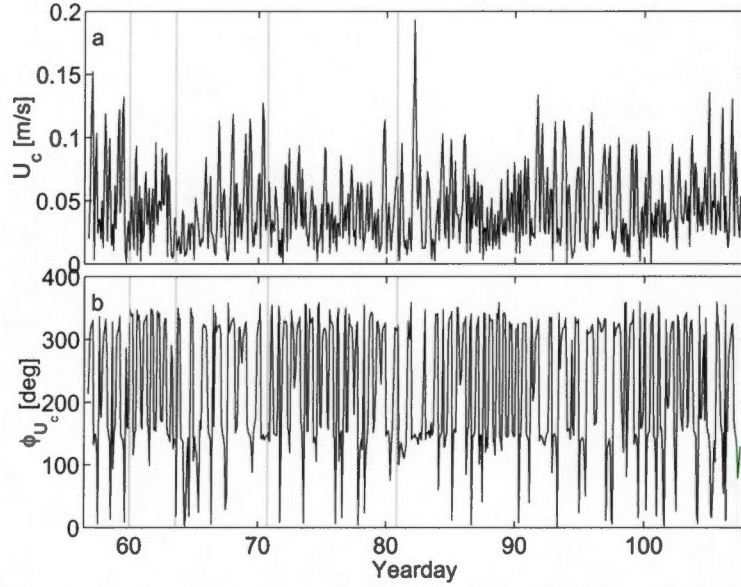


Figure 4: Time series of: (a) average current speed measured by the ADV, and (b) average current direction (0 is magnetic North). Dotted lines indicate the position of storm peaks.

attenuation. The noise threshold was set to 2 bits, as identified in the data during calm conditions. This value is higher than the precision of the pressure data, identified as $\pm 0.15\%$ of the full scale depth (70 m).

Tidal-peak mean current velocities were approximately 0.1 m/s, oriented generally south-east/north-west, Figure 4. The mean current was measured by the ADV at approximately 30 cm above the bed. Mean current speed, U_c is defined as $U_c = \sqrt{U^2 + V^2}$ where U is the x component of the current and V is the y component. The direction of the average current, ϕ_{U_c} is defined as $\phi_{U_c} = -\tan_2^{-1}(V/U) + \phi_M - 90^\circ$ where ϕ_M is the compass heading and \tan_2^{-1} is the four quadrant arctangent. The 90° correction is applied as the compass is aligned with the $+y$ axis. In agreement with Li *et al.* [1999], this data set shows that the mean currents were suppressed at the peaks of storms (e.g. yeardays 60 and 64.).

Storm-peak significant wave velocities ranged from 0.2 to 0.6 m/s, and were generally in the north/northwest direction, Figure 5. The significant wave velocity, U_{wo} is defined as $U_{wo} = 2\sqrt{\sigma_u^2 + \sigma_v^2}$, where σ_u^2 is the 2nd order moment of the x component of the velocity.

2.4 Mobile Layer Depth

One of the objectives of this analysis was to determine the maximum depth of the mobile layer for the experiment and compare the present observations to predictions by Li *et al.* [1999]. The maximum depth of the mobile layer is estimated from the greater of the bedform amplitude or the seafloor elevation change.

Seafloor elevation changes were estimated from the vertically oriented ABS's and the ADV's. The seafloor was identified as the position of the maximum backscatter amplitude. A time series of the distance from the acoustic transducers to the seafloor, d_b , indicates that changes in elevation of approximately 15 and 12 cm occurred on yeardays 58 and 62 respectively, Figure 6. Bedform heights may be inferred from the difference in elevation for the two ADV's. Maximum differences approach 10 cm, indicating a bedform amplitude of 5 cm.

Frame movement may cause an apparent change in the distance to the bed. Estimates of the pitch and roll of the instrument frame were measured by a tilt sensor which was located in the main pressure case.

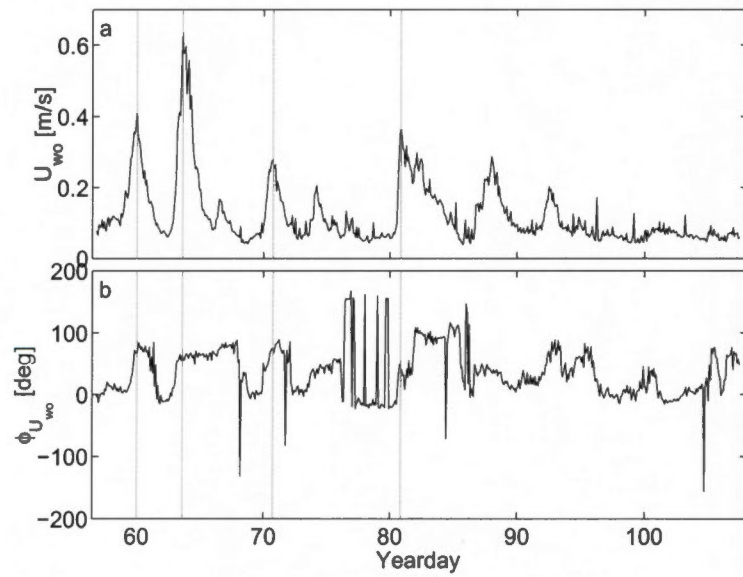


Figure 5: Time series of: (a) average significant wave velocity, and (b) average wave direction.

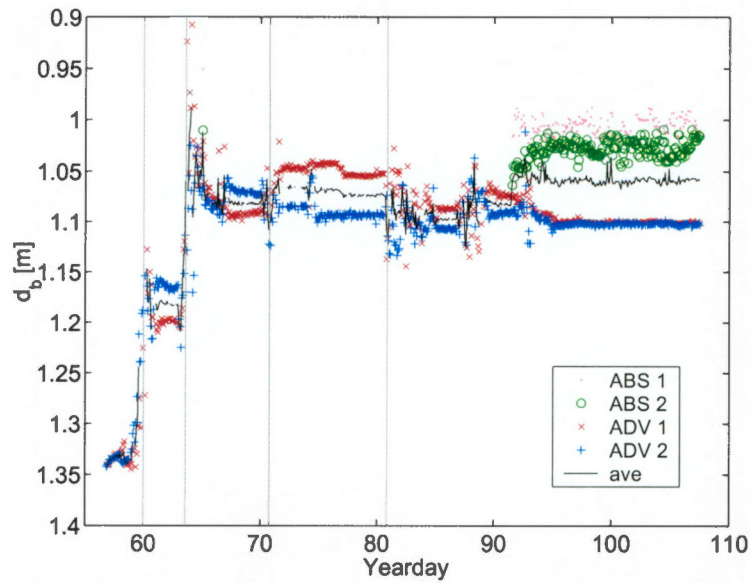


Figure 6: Time series of distance from the acoustic transducers to the seafloor. The average of all 4 time series is indicated by the solid line.

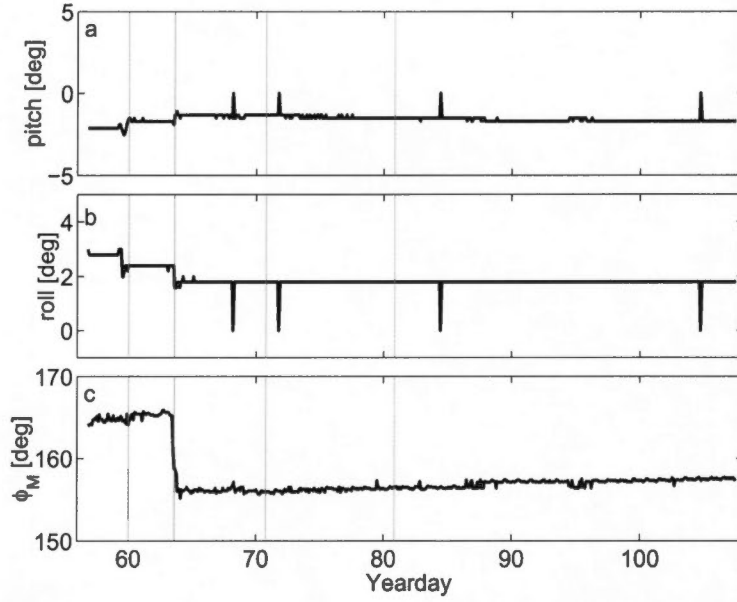


Figure 7: Time series of the instrument frame pitch, roll and compass heading.

Time series of pitch, roll and compass reading show modest changes (<1 deg) in the pitch and roll during the deployment, Figure 7. However, during the storm on yearday 64 the compass heading changed by approximately 10 degrees.

A least-squares fit by *Li et al.* [1999] of the data collected during previous deployments in 1996 and 1997 predicted the mobile layer depth, d_m as

$$d_m = 0.061H_s \quad (1)$$

where H_s is the significant wave height. This empirical result predicts a mobile layer depth of 13 and 18 cm respectively for a significant wave heights of 2.2 and 2.9 m respectively. The present observations of 15 and 12 cm are within 30% of the predictions.

2.5 Bedforms

Small bedforms were observed using the digital video camera data, an example of which is shown in Figure 8. Two short clips of video data were collected during each burst: a 1 second clip at the beginning of the burst and a 7 second clip at the end. The field of view was approximately 0.5×0.7 m. Approximate estimates of bedform wavelength were determined from video images by counting the number of ripple crests and dividing by the width, 0.7 m. Figure 9a shows that at times there was only 1 ripple present in the field of view of the camera, indicating large-wave ripples with a minimum wavelength of 0.7 m.

2.6 Sediment Transport Mode

Longer video clips were visually analyzed to determine if bedload or suspended load transport was evident, Figure 9. Bedload transport was observed during all storms, even lower energy storms. Suspended load transport was only visible during some of these times, mainly during higher wave energy conditions.

Large numbers of flocs suspended in the water column were visible in the video data. During low wave energies between the storms on yeardays 65 and 71, the concentration of flocs was dense enough to at times



Figure 8: Frame capture of a digital video clip showing small bedforms on yearday 61, at 2:54 am.

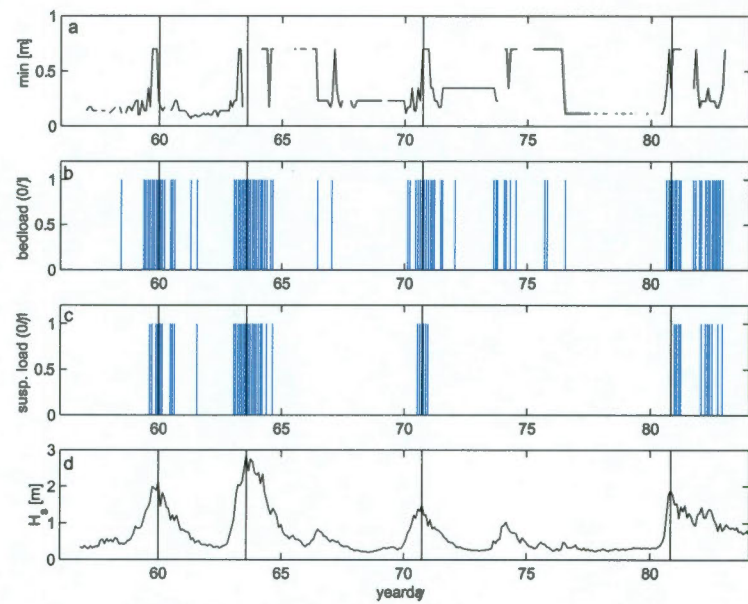


Figure 9: Time series of: (a) estimated ripple wavelength; (b) bedload transport mode; (c) suspended transport mode and (d) significant wave height.

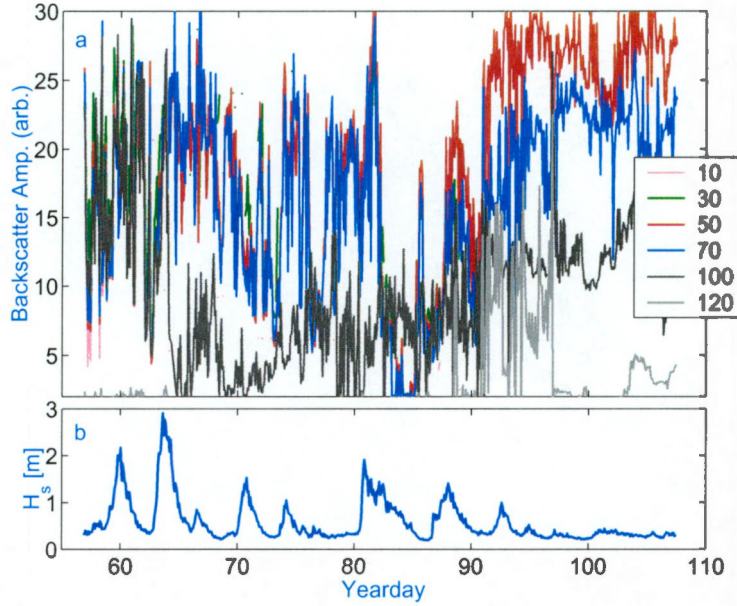


Figure 10: Time series of: (a) backscatter amplitude from the OBS's and (b) significant wave height. The height (in cm) of the OBS relative to a reference level close to the seafloor are shown in the legend.

obscure the seafloor. On yearday 68 the flocs settled out of the water column and formed matts in the ripple troughs. Increasing wave energy broke up the matts and dispersed the flocs.

2.7 Sediment Suspension

Suspended sediment levels were measured by OBS's during most of the deployment and by ABS's for 15 days near the end of the experiment. Figure 10 shows that OBS sensors had elevated levels during storm conditions. Higher levels of the OBS during calmer conditions suggest that the OBS is sensitive to flocs. Near the end of the experiment during relatively calmer wave conditions, the OBS levels are uniformly high, which may have been related to the presence of water in the pressure case. The current meter electronics were in the same pressure case as the OBS and did not record any data after yearday 90. The ABS sensors recorded data near the end of the experiment, Figure 11. There were higher suspended sediment levels on yearday 93 when the significant wave height approached 1 m. However the ABS response was generally weak, consistent with lower energy conditions.

3 Predictions by SEDTRANS96

SEDTRANS96 is a combined wave-current bottom boundary layer model that predicts bed shear stresses, suspended sediment transport rates, bedload sediment transport rates and bedload transport direction [Li and Amos, 2001]. Measurements of depth, current velocity, current direction, wave direction, wave period and grain diameter were input into the model (Appendix A). Additional input parameters were a sediment grain density of 2.65 g/cm^3 , fluid density of 1.025 g/cm^3 , bed slope of zero, and initial flat bed. Predicted sediment transport rates from SEDTRANS96 are shown in Table A-1 and predicted bottom boundary layer parameters are in Table A-2. Maximum predicted sediment transport rates were 4.7 g/m/s for bedload in a direction of 122 degrees and 0.9 g/m/s for suspended load on yeardays 82 and 63 respectively.

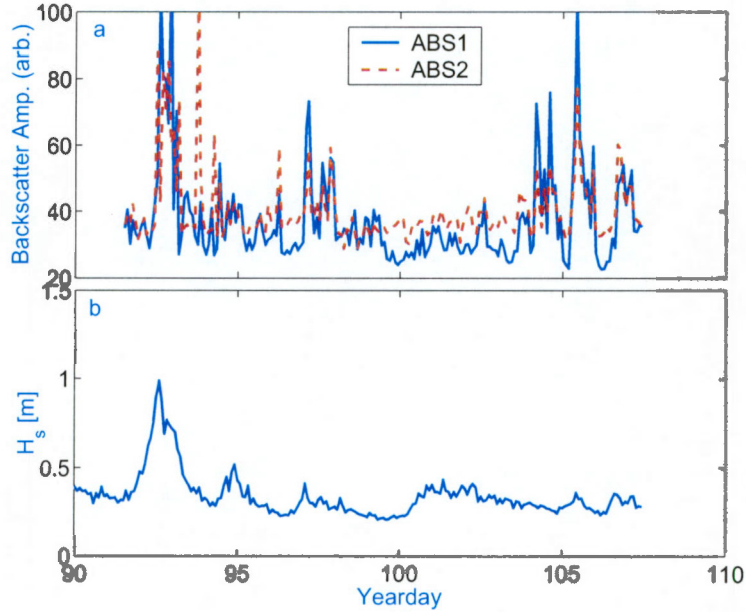


Figure 11: Time series of: (a) backscatter amplitude from ABS1 and ABS2 at approximately 50 cm above the bed and (b) significant wave height.

4 Acknowledgments

The authors would like to thank Bob Murphy, Fred Jodrey, Angus Robertson, Tony Atkinson and Owen Brown for providing field, technical and laboratory assistance. We would also like to thank Ned King for reviewing this report.

References

- Heffler, D. E., A dynamic instrument for sediment dynamics, in *Proc. of Oceans '96, IEEE*, pp. 728–732, 1996.
- Li, M. Z., and C. L. Amos, Sedtrans: the upgraded and better calibrated sediment-transport model for continental shelves, *Comp. GeoSci.*, 27, 619–645, 2001.
- Li, M. Z., C. L. Amos, and D. E. Heffler, Hydrodynamics and seabed stability observations on sable island bank: A summary of the data for 1996/1997, *Tech. Rep. 2997*, Geological Survey of Canada, 1999.

A SEDTRANS96 inputs and predictions

Table A-1 lists average wave and current parameters for each burst. These parameters were input into a sediment transport model SEDTRANS96. Predictions of sediment transport rates and boundary layer parameters are given in Tables A-1 and A-2. The following list describes the column headings.

δ_{cw} thickness of the wave-current boundary layer [cm]

η_p predicted ripple height [cm]

λ_p predicted ripple wavelength [cm]
 ϕ_u wave direction [deg]
 ϕ_U current direction [deg]
 A_{ABS} , suspended sediment levels from the ABS₁ [arb]
 A_{OBS} suspended sediment levels from OBS₄ [arb]
 A_b near-bed wave orbital amplitude [m]
 H_s significant wave height [m]
 Q_b Einstein-Brown estimate of mean sediment transport rate [$\text{g m}^{-1} \text{s}^{-1}$]
 $Q_{b,dir}$ direction of mean sediment transport rate [deg]
 Q_s mean suspended load sediment transport rate [$\text{g m}^{-1} \text{s}^{-1}$]
 T_w energy weighted wave period [s]
 U mean current speed [cm/s]
 f_{cw} combined wave-current friction factor
 u_{*cs} skin friction current shear vel [cm/s]
 u_{*c} total current shear vel [cm/s]
 u_{*cw} total combined wave-current shear vel [cm/s]
 u_{*cws} skin friction combined wave-current shear vel [cm/s]
 u_{*w} total wave shear vel [cm/s]
 u_{*ws} skin friction wave shear vel [cm/s]
 u_b near-bed maximum wave orbital velocity [m/s]
 z_0 inner layer bottom roughness [cm]
 z_{0c} apparent bottom roughness above the wave boundary layer [cm]

